

Coexistence of ferromagnetic and antiferromagnetic order in Mn-doped Ni₂MnGaJ. Enkovaara,^{1,*} O. Heczko,² A. Ayuela,¹ and R. M. Nieminen¹¹Laboratory of Physics, P.O. Box 1100, Helsinki University of Technology, FIN-02015 HUT, Finland²Laboratory of Biomedical Engineering, P.O. Box 2200, Helsinki University of Technology, FIN-02015 HUT, Finland

(Received 14 April 2003; published 16 June 2003)

Ni-Mn-Ga is interesting as a prototype of a magnetic shape-memory alloy showing large magnetic-field-induced strains. We present here results for the magnetic ordering of Mn-rich Ni-Mn-Ga alloys based on both experiments and theory. Experimental trends for the composition dependence of the magnetization are measured by a vibrating sample magnetometer in magnetic fields of up to several tesla and at low temperatures. The saturation magnetization has a maximum near the stoichiometric composition and it decreases with increasing Mn content. This unexpected behavior is interpreted via first-principles calculations within the density-functional theory. We show that extra Mn atoms are antiferromagnetically aligned to the other moments, which explains the dependence of the magnetization on composition. In addition, the effect of Mn doping on the stabilization of the structural phases and on the magnetic anisotropy energy is demonstrated.

DOI: 10.1103/PhysRevB.67.212405

PACS number(s): 75.30.Cr, 75.50.Cc, 75.50.Ee

Ni-Mn-Ga alloys have unique magnetoelastic and magnetoplastic properties, which make them highly interesting for many technological applications such as smart actuator materials.^{1,2} The material properties are sensitive to the actual composition.³ The best alloys to date are rich in Mn and poor in Ga with respect to the perfect Ni₂MnGa stoichiometry. In particular, a shape-memory alloy around Ni₂Mn_{1.25}Ga_{0.75} composition shows excellent magnetoelastic properties with strains of up to 10% under moderate magnetic fields. Its recent discovery has inspired substantial experimental and theoretical activity.⁴ Typically these materials are produced by several techniques, such as directional solidification and Bridgman growth,⁵ and one has also been able to grow them epitaxially on GaAs substrates.⁶ Apart from the composition dependence, the ordering of the atoms in the different sublattices within the $L2_1$ structure, as depicted in Fig. 1, is not yet well understood. A thorough theoretical investigation of the phase equilibrium is also lacking, and additionally many details about bonding and ordering in this system are not yet well understood.⁷

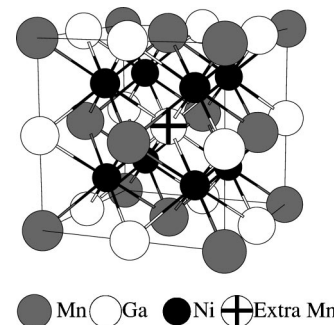
In order to facilitate a technological breakthrough, the magnetic properties of this material should be explored in detail. For the perfect stoichiometric case, experimental as well as theoretical works agree on the saturation magnetization of $4.1\mu_B$ per f.u.^{8,9,11} For Mn-rich alloys with a constant 50% Ni content, the extra Mn atoms substitute Ga atoms in the Ga sublattice. The Mn atoms would contribute by $3.5\mu_B$ to the total magnetic moment as described in Refs. 8, 9, and 11. However, addition of Mn does not correlate with an increase in the overall magnetization, as shown by the experimental results below. Thus there is a serious difference between the experimental results and the expected trends. In this paper we address this problem with a combined experimental and theoretical study.

Most of the alloys used to date have been developed with a metallurgical approach. In contrast, we use alloy theory in order to identify the phases,⁹ to understand the martensitic phase-transition mechanism,^{9,10} and to predict the possible candidates for future materials.¹¹ Here we show a nearly perfect agreement between theory and experiment considering

magnetic order in alloying with Mn atoms. As a bonus we also provide a microscopic explanation for further stabilization of the martensite phases appearing at low temperature. Finally, we report the calculated magnetic anisotropy energy which deviates from the results based on the average electronic concentration.

The details of the experiments are the following. Various alloys with compositions close to stoichiometric Ni₂MnGa were melted from pure elements and nearly single-crystal ingots were produced by a modified Bridgman method. The as-cast ingots were homogenized at 1000 °C. The saturation magnetization is studied as a function of the composition. The chemical composition of the samples is determined by energy dispersive spectroscopy. While the content of Ni remains an almost constant 50%, the content of Mn spans the range between 19% and 34%. The magnetization curves are measured with a vibrating sample magnetometer (VSM) up to a field of 2 T and with a superconducting quantum interference device magnetometer up to a 5-T field. Measurements are made for several temperatures down to 10 K (see the inset of Fig. 2). The spontaneous saturation magnetization is determined by extrapolation to the zero-field limit from the magnetization measurements at 10 K.

For modeling, we use the generalized-gradient approximation^{12,13} of spin-density-functional theory. For the total-energy calculations, we use both a full-potential linearized augmented plane-wave method¹⁴ and a pseudopotential

FIG. 1. $L2_1$ supercell of Ni₂Mn_{1.25}Ga_{0.75}.

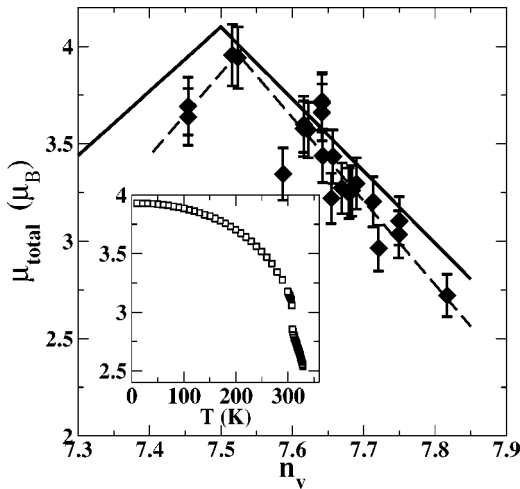


FIG. 2. Saturation magnetization vs the average number of valence electrons per atom (n_v). The dashed line is a linear fit to the experimental data and the solid line is the theoretical prediction. The inset shows the temperature dependence of the magnetization in the composition $\text{Ni}_{1.99}\text{Mn}_{1.16}\text{Ga}_{0.85}$.

scheme.^{15,16} As shown in previous calculations, the Mn magnetic moment is high, and we have confirmed the pseudopotential validity by comparing full-potential calculations with pseudopotential calculations. In this particular case, the pseudopotential treatment is valid concerning the magnetic ordering and accurate enough for dealing with the main features of the structural phase transitions in these materials. The details of these results will be discussed elsewhere.¹⁷ The substitutional and magnetic alloying is treated by replacing one Ga atom with a Mn atom in the 16-atom $L2_1$ supercell (Fig. 1), resulting in the composition $\text{Ni}_2\text{Mn}_{1.25}\text{Ga}_{0.75}$. The magnetic moment of the extra Mn atom is allowed to have both parallel and antiparallel alignment with respect to the other Mn atoms, collinearly ordered, and the total energy is minimized with respect to each magnetic configuration.

Figure 2 shows the magnetization measurements of $\text{Ni}_2\text{Mn}_{1+x}\text{Ga}_{1-x}$ alloys as a function of the average valence electron concentration n_v . The average concentration is measured by the electron-to-atom ratio where Ni contributes ten, Mn seven, and Ga three valence electrons. The temperature dependence of the magnetization (see the inset of Fig. 2) has been measured at the field $H=2$ T, which is larger than the saturation field. The saturation magnetization shows a peak at 7.5 valence electrons/atom corresponding to the perfect stoichiometric Ni_2MnGa alloy. The magnetic moment has a value of about $4\mu_B$ per f.u. which is in agreement with previous experimental data⁸ on stoichiometric Ni_2MnGa as well as with the first-principles calculations.^{9,11} The experimental data show that the magnetic moment decreases when the electronic concentration increases over 7.5. This finding is in agreement with the data of Ref. 18 which have been collected from several sources and show smaller values for the magnetization since the saturation is not well guaranteed. This is because measurements are made with either a low field or at high temperatures.

In order to explain the experimental results above and to gain insight into the precise magnetic structure, we present

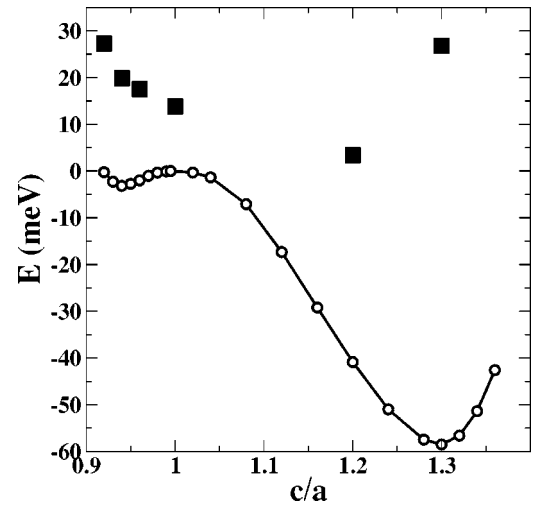


FIG. 3. Calculated total energy of $\text{Ni}_2\text{Mn}_{1.25}\text{Ga}_{0.75}$ per formula unit as a function of the tetragonal distortion c/a ratio. Circles mark the antiferromagnetic alignment of the extra Mn and squares mark the ferromagnetic alignment.

the following theoretical results. As a first step, let us analyze the magnetic properties based on the average electron concentration within the rigid-band approximation. It is found that the Mn moment remains constant but the Ni moment decreases linearly with increasing electron concentration. This picture cannot therefore explain the experimental decrease of the magnetization when lowering electron concentration below 7.5. Also, the decrease of the magnetic moment per Ni atom is only $0.1\mu_B(n_v)^{-1}$ which is smaller than that in the experiments. When the extra Mn atom is included explicitly in the calculation, the configuration with *antiparallel* alignment of Mn moments is energetically favorable as seen in Fig. 3. An analysis of the local Mn magnetic moment gives a nearly constant value of around $3.5\mu_B$ regardless of the alignment, so that the total magnetic moment has a value of $5.0\mu_B$ for the ferromagnetic configuration, and a value of $3.6\mu_B$ for the antiferromagnetic one. The latter value is in good agreement with the experiments.

The variation of the magnetization with the composition can be estimated with a simple model. As the extra Mn atoms couple antiferromagnetically with the neighboring Mn atoms, every additional Mn atom decreases the total magnetic moment by $3.5\mu_B$. The total magnetic moment of $\text{Ni}_2\text{Mn}_{1+x}\text{Ga}_{1-x}$ is then given by $\mu_{total} = 2\mu_{Ni} + (1 - |x|)3.5\mu_B$ where the Ni moment μ_{Ni} is varied around the stoichiometric value $0.3\mu_B$ with the electron concentration according to the rigid-band results. One should note that the variation of the Ni moment affects only slightly the total moment whose variation is determined mostly by Mn. The linear fit of the experimental data agrees well with the line predicted by the theory, assuming a constant 50% content of Ni.¹⁹ The reason for the peak of the saturation magnetization with electron concentration around 7.5, as well as the decreasing trend of the saturation magnetization, are identified here in a natural way. We can conclude that the Mn atoms substituted at the Ga sites are antiferromagnetically coupled to the Mn atoms at Mn sites. In addition to the experimental

compositions, with an approximately constant 50% Ni content, we check the magnetic moments also in $\text{Ni}_{1.75}\text{Mn}_{1.25}\text{Ga}$, where one Ni atom is replaced by Mn in the previous 16-atom supercell. The results show that also in this case the additional Mn favors similar antiferromagnetic alignment, but with a local magnetic moment of $0.7\mu_B$. These findings can be reasoned by the tendency of close Mn atoms to favor an antiferromagnetic alignment, typical for several Mn compounds.²⁰ The interesting new feature here is the coexistence of ferromagnetic and antiferromagnetic Mn-Mn interactions in the same alloy.

It should be pointed out that during cooling the alloys undergo martensitic transformations, in some cases actually several intermartensitic transformations from so-called 5 M to 7 M and to nonmodulated martensite.²¹ For instance, in the inset of Fig. 2, an abrupt jump in the curve indicates the austenite-martensite transformation at about 305 K. During the transformation the saturation magnetization can change by 10%, but the low-temperature moment remains nearly equal as shown in previous calculations.⁹ The antiferromagnetic alignment is energetically favorable also in the martensitic phase (Fig. 3), so that the phase transitions do not affect the above conclusions.

We next discuss the existence of martensitic phases for the desirable compositions. In the stoichiometric alloy total-energy calculations show two energy minima with tetragonal structures $c/a \sim 0.94$ and $c/a \sim 1.3$.⁹ However, when the Mn doping is modeled with the rigid-band approximation the energy minimum at $c/a \sim 0.94$ disappears. In Fig. 3 we present total-energy calculations beyond the rigid-band approximation where the additional Mn is explicitly included. There is now a stable structure at $c/a \sim 0.94$ both with parallel and antiparallel alignments of the extra Mn, but the antiferromagnetic coupling clearly stabilizes the minimum over the ferromagnetic case. When taking into account also orthorhombic distortions with the antiferromagnetically aligned extra Mn, we find a new energy minimum with $c/a \sim 0.93$ and $b/a \sim 0.97$. The energy of this orthorhombic minimum is between the two tetragonal minima, so that the theoretical order of the phases agrees with the experimental findings.²¹ We can conclude that the structural and magnetic ordering beyond simple electronic averaging are important in stabilizing some of the phases.

Another key property in magnetism is the magnetic anisotropy energy. Previously the composition dependence of

the magnetic anisotropy energy has been analyzed by taking into account only the average electron concentration.¹⁰ It is shown in Ref. 10 that the magnetic anisotropy energy decreases with increasing electron concentration, in agreement with experiments. Since the doping changes also the local structural and magnetic properties we refine here the analysis and calculate the magnetic anisotropy with the extra Mn explicitly included. With average electron concentration corresponding to $\text{Ni}_2\text{Mn}_{1.25}\text{Ga}_{0.75}$ composition the anisotropy energy of the $c/a = 0.94$ structure is $50 \mu\text{eV}$ per f.u. When including the extra Mn explicitly the magnetic anisotropy energy is $150 \mu\text{eV}$ for the ferromagnetic alignment and $100 \mu\text{eV}$ for the antiferromagnetic one, where the last value is in good agreement with the experimental one of $90 \mu\text{eV}$.²² It is seen that even though simple averaging of electrons can reproduce the correct trends, the structural and magnetic ordering are important for quantitative determination of the magnetic anisotropy energy.

In conclusion, the magnetic properties of Mn-doped Ni_2MnGa alloys are measured for several concentrations and calculated for those showing interesting magnetoelastic properties. Experimentally, we see that doping has a strong effect on the saturation magnetization. The computational results within the density-functional theory show that the extra Mn is antiferromagnetically aligned to the other atoms in the $L2_1$ lattice and a comparison of the experimental and the theoretical magnetizations confirms this picture. The ordering of the extra Mn is shown to affect also the appearance of the tetragonal and orthorhombic structures and the magnetic anisotropy energy. The main result of this work, the magnetic alignment of the extra Mn, could serve as an impetus for further work on the ordering issue. For example, the interaction of frustrated magnetic sublattices in Ni-Mn-Ga should be revealed by using sublattice-sensitive probes.

This work has been supported by the Academy of Finland (Centers of Excellence Program 2000–2005), by the National Technology Agency of Finland (TEKES), and the consortium of Finnish companies (AdaptaMat Oy, Metso Oyj, Outokumpu Research Oy). O.H. thanks Miroslav Marysko and Milos Jirsa from the Institute of Physics, Academy of Science, the Czech Republic, for help with the magnetization measurements. Computer facilities of the Center for Scientific Computing (CSC), Finland, are greatly acknowledged. We thank A. Foster for the careful and critical reading of the manuscript.

*Electronic address: jen@fyslab.hut.fi

¹A.N. Lavrov, S. Komiya, and Y. Ando, *Nature (London)* **418**, 385 (2002).

²R. C. O'Handley, *Modern Magnetic Materials: Principles and Applications* (Wiley, New York, 1999). See also <http://www.adaptamat.fi/materials.html>

³V.A. Chernenko, *Scr. Mater.* **40**, 523 (1999); S.J. Murray, M. Farineli, C. Kantner, J.K. Huang, S.M. Allen, and R.C. O'Handley, *J. Appl. Phys.* **83**, 7297 (1998); K. Tsuchiya, A. Ohashi, D. Ohtoyo, H. Nakayama, M. Umemoto, and P.G. McCormick, *Mater. Trans., JIM* **8**, 938 (2000).

⁴See, for instance, V.V. Khovailo, T. Takagi, J. Tani, R.Z. Levitin,

A.A. Cherechukin, M. Matsumoto, and R. Note, *Phys. Rev. B* **65**, 092410 (2002); G.H. Wu, W.H. Wang, J.L. Chen, L. Ao, Z.H. Liu, W.S. Zhan, T. Liang, and H.B. Xu, *Appl. Phys. Lett.* **80**, 634 (2002); C. Jiang, G. Feng, and H. Xu, *ibid.* **80**, 1619 (2002).

⁵O. Heczko, A. Sozinov, and K. Ullakko, *IEEE Trans. Magn.* **36**, 3266 (2000); O. Heczko, K. Jurek, and K. Ullakko, *J. Magn. Mater.* **226**, 996 (2001); S.J. Murray, M.A. Marioni, A.M. Kukla, J. Robinson, R.C. O'Handley, and S.M. Allen, *J. Appl. Phys.* **87**, 5774 (2000).

⁶J.W. Dong, L.C. Chen, J.Q. Xie, T.A.R. Müller, D.M. Carr, C.-J. Palmström, S. McKernan, Q. Pan, and R.D. James, *J. Appl.*

- Phys. **88**, 7357 (2000).
- ⁷R.W. Overholser, M. Wuttig, and D.A. Neumann, *Scr. Mater.* **40**, 1095 (1999).
- ⁸P.J. Webster, K.R.A. Ziebeck, S.L. Town, and M.S. Peak, *Philos. Mag. B* **49**, 295 (1984).
- ⁹A. Ayuela, J. Enkovaara, and R.M. Nieminen, *J. Phys.: Condens. Matter* **14**, 5325 (2002).
- ¹⁰J. Enkovaara, A. Ayuela, L. Nordström, and R.M. Nieminen, *Phys. Rev. B* **65**, 134422 (2002); *J. Appl. Phys.* **91**, 7798 (2002).
- ¹¹A. Ayuela, J. Enkovaara, K. Ullakko, and R.M. Nieminen, *J. Phys.: Condens. Matter* **11**, 2017 (1999).
- ¹²J.P. Perdew, J.A. Chevary, S.H. Vosko, K.A. Jackson, M.R. Pederson, D.J. Singh, and C. Fiolhais, *Phys. Rev. B* **46**, 6671 (1992).
- ¹³J.P. Perdew and Y. Wang, *Phys. Rev. B* **45**, 13 244 (1992), and references therein.
- ¹⁴P. Blaha, K. Schwarz, and J. Luitz, computer code WIEN97, an improved and updated Unix version of the copyrighted WIEN code (Vienna University of Technology, Vienna, Austria, 1997); [P. Blaha, K. Schwarz, P. Sorantin, and S.B. Trickey, in *Comput. Phys. Commun.* **59**, 399 (1990) is used here.]
- ¹⁵G. Kresse and J. Furthmüller, *Phys. Rev. B* **54**, 11 169 (1996); computer code VASP, the Guide (Vienna University of Technology, Vienna, Austria, 1999); <http://tph.tuwien.ac.at/~vasp/guide/vasp.html>
- ¹⁶G. Kresse and D. Joubert, *Phys. Rev. B* **59**, 1758 (1999).
- ¹⁷J. Enkovaara, J. Jalkanen, J. Imppola, A. Ayuela, R. M. Nieminen, and L. Nordstrom (unpublished).
- ¹⁸X. Jin, M. Marioni, D. Bono, S.M. Allen, R.C. O'Handley, and T.Y. Hsu, *J. Appl. Phys.* **91**, 8222 (2002).
- ¹⁹In reality the Ni content varied from 48 to 53 at. %. Most of the scatter is, however, due to errors in the chemical analysis. Also, the Mn moment may vary slightly, giving small variation from the exact linear behavior.
- ²⁰J. Kübler, A.R. Williams, and C.B. Sommers, *Phys. Rev. B* **28**, 1745 (1983).
- ²¹O. Heczko, N. Lanska, O. Soderberg, and K. Ullakko, *J. Magn. Mater.* **242–245**, 1446 (2002).
- ²²L. Straka and O. Heczko, *J. Appl. Phys.* **93**, 8636 (2003).